Article:

Measuring Contact Area in a Sliding Human Finger-Pad Contact

X. Liu[1], M.J. Carré[2], Q. Zhang[3], Z. Lu[4], S.J. Matcher[4], R. Lewis[2]

(1) Engineering and Technology Research Institute, Liverpool John Moores University, Byrom Street, Liverpool, L3 3AF.

(2) The Department of Mechanical Engineering, The University of Sheffield, Mappin Street, Sheffield, S1 3JD.

(3) The Department of Electronic and Electrical Engineering, Liverpool John Moores University, Byrom Street, Liverpool, L3 3AF.

(4) The Department of Materials Science and Engineering, The University of Sheffield, Mappin Street, Sheffield, S1 3JD.

* Corresponding author. Tel: +44 (0)114 222 7838; Fax: +44 (0) 114 222 7890; Email address: roger.lewis@sheffield.ac.uk

ABSTRACT

Background/Purpose: The work outlined in this paper was aimed at achieving further understanding of skin frictional behaviour by investigating the contact area between human finger-pads and flat surfaces.

Methods: Both the static and the dynamic contact areas (in macro- and micro-scales) were measured using various techniques, including ink printing, Optical Coherence Tomography (OCT) and Digital Image Correlation (DIC).

Results: In the studies of the static measurements using ink printing, the experimental results showed that the apparent and the real contact area increased with load following a piecewise linear correlation function for a finger-pad in contact with paper sheets. Comparisons indicated that the OCT method is a reliable and effective method to investigate the real contact area of a finger-pad and allow micro-scale analysis. The apparent contact area (from the DIC measurements) was found to reduce with time in the transition from the static phase to the dynamic phase while the real area of contact (from OCT) increased.

Conclusions: The results from this study enable the interaction between finger-pads and contact object surface to be better analysed, and hence improve the understanding of skin friction.

Keywords: Skin tribology, Contact area, Ink printing method, OCT, DIC

1. INTRODUCTION

Since scientists have realised the importance of skin friction in human daily tasks, such as feeling, grasping, lifting and manipulating, the behaviour of skin friction has been examined in many studies. The frictional behaviour of skin is complex and involves different interactions between skin and substrates. It is generally described by the same theoretical friction concepts used for rubber due to the similarity in the viscoelastic properties. Those physical reactions are the results of many different mechanisms, such as interfacial shear, adhesion, capillary action and viscoelastic hysteresis [1, 2]. It is believed that a simple model (Amonton's law) cannot provide an accurate description for the skin friction. According to Bowden & Tabor, in dry sliding contacts, the skin friction is generally modelled as viscoelastic deformation forces of microscopical asperities in contact and can be expressed by a two-term model [3]. In this case, the friction of skin is assumed to be only associated with an adhesion mechanism, for dry and smooth surfaces, while the deformation is normally ignored [4-6]. In the case of dry sliding friction on a surface with high roughness, skin friction is reported to depend on the adhesion mechanism and hysteresis [7]. In a recent study, Tomlinson et al. [8] has conducted experimental work on skin friction for a human finger-pad in contact with fine rough surfaces. They concluded that the skin friction force can be analysed in terms of an adhesion force, a hysteresis mechanism and an interlocking mechanism.

Previous studies have revealed that contact area is the key influencing parameter in a skin/counterface contact [3, 7, 9-18]. For example, Bowden & Tabor [3] investigated the effect of load on the friction of polymers, and indicated that the contact area is the major factor affecting the friction. They also concluded that the friction of visco-elastic materials is ascribed to the adhesion mechanism in the case that the tested materials experience slow movements. Furthermore, they derived a simple model to explain the relationship between the friction force and the contact area, expressed as: $F = \tau \times A_{re}$, where τ is the shear strength and A_{re} is the real area of contact. The contact area was shown to be proportional to the normal load applied. This observation is in good agreement with the results in other studies [19-22]. Tomlinson [21], however, reported that the contact area obeys a two part linear relationship. The initial linear part is believed to be associated with the bulk properties of finger and the secondary part is attributed to the deformation of the finger ridges and asperities. The related transition point occurs at friction force of about 2 N.

For those tests where hemispheres slide against skin, there are two different deformations, i.e., pure plastic deformation and pure elastic deformation, both of which are considered to be involved in the contact area [23-24]. The real contact area is expected to be directly proportional to the normal load in the case of pure plastic contact. On the other hand, different from the plastic contact, the real contact area is proportional to the normal load to the power of 2/3 in the case of pure elastic contact, which is in accordance with the Hertz's equation [25]. El-shimi [26] suggested that the contact area for visco-elastic materials is likely to be dependent on the elastic deformation rather than the plastic deformation. However, Han et al. [11] indicated that the

Hertz's model is only applicable for the case of a hemispherical probe sliding on deformable materials. As human fingers do not experience smooth spherical contact, Hertz's model cannot be used to accurately estimate the contact area between finger-pads and contact surfaces. They also suggested that the change in the contact area with load follows a power-law relationship.

Although, as can be seen from the discussion above, the investigation of the contact area between finger-pad skin and object interfaces is critical for characterizing the frictional behaviour of skin, it is difficult to measure the real contact area due to the limited techniques available, however. As it is known, human finger-pad skin is not smooth and is covered with a pattern of ridges. These ridges do not permit skin to contact surfaces completely, even at high load (see Figure 1).

There have been several studies measuring the contact area of finger skin in contact with objects using a variety of techniques. Ink printing [19-21] and optical methods [21, 22, 27] have been used, both of which can give the ridge contact area and the macro nominal contact area. An electrical resistance method (only useful for studying contact area changes) [21] and CCD camera studies (for nominal contact area only) [7, 11] have also been used. In the ink printing study carried out by Tomlinson [21] the contact area of the examined finger was reported to increase with load following a linear relationship, and the ratio of the ridges area to the total area was between 0.38 and 0.5. In the similar studies of Childs & Henson's [19], they found that the apparent contact area increased with load (up to 2 N). This type of measurement is affected by spread of the ink post printing and is thought to give higher than would be expected results. The other methods show similar trends and have both advantages and disadvantages over the ink printing approach, but all are limited to static measurements or to macro nominal contact area measurements only. Optical Coherence Tomography (OCT) has been used recently to investigate more closely the changes in ridge contact [28-30]. While only used so far for static measurements, this does has the possibility of being used for dynamic measurements which is a key next step in the development of tribological models of the finger-pad. More details of the data from the methods mentioned will be given in discussing the outcomes of the present work.

The objective of this paper is to experimentally investigate static and dynamic contact areas (in macro- and micro- scales) between human finger-pads and paper, as well as a smooth glass surface using various methods, including an ink printing method, an OCT method and a Digital Image Correlation (DIC) method.
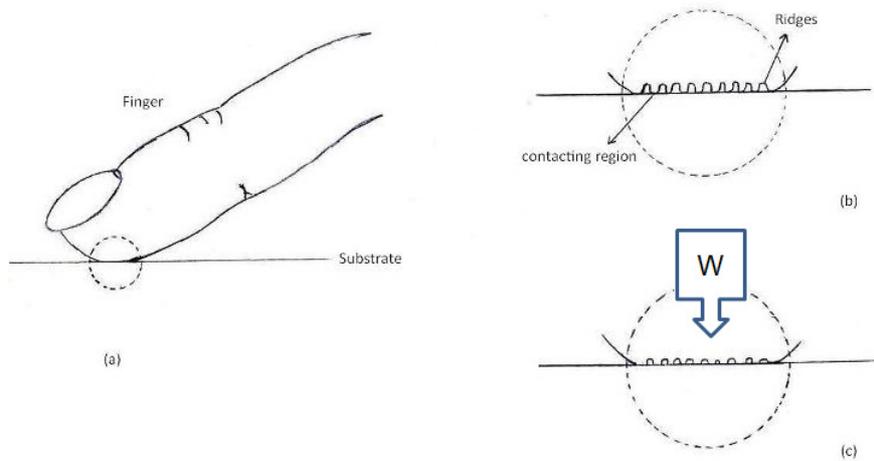
Figure 1: A finger-pad in contact with a substrate; (b) micro-scale of contact region without significant load, and (c) micro-scale of contact region with load W.

## 2. EXPERIMENTAL DETAILS

2.1 Measurements of Static Contact Area

2.1.1   Ink Printing Method

In this part of the study, static measurements were performed on a multi-axis force plate (HE6X6 from Advanced Mechanical Technology Ltd.) (see [28] for details of previous use). A white paper sheet was attached on the top surface of the force plate, which allowed participants to record their fingerprints by pressing down ink stained finger-pads. To investigate the effect of the normal load on the contact area, the right index finger-pad of a 25 year old female was used. Firstly, the finger-pad was pressed onto an ink sponge so that a thin film of ink covered the surface of the skin. The stained finger-pad was then pressed onto the white paper sheet at an angle of 25°– 40° with various loads (in the range of 0.5 ~ 24.5 N) to produce fingerprints. In order to avoid the issues with ink drying and image blurring, the participant was requested to conduct the test quickly. The time delay between finger-pad staining and the contact area measurement was approximately 2–5 seconds. All fingerprints produced were recorded using a digital camera.

All fingerprints obtained were then transferred to a PC and were further analysed using an image-processing algorithm (written using Matlab), developed to calculate the total apparent and real contact areas respectively. A sample output is shown in Figure 2, in which the shape of the index fingerprint at angles between 15° and 45° could be assumed as an ellipse, in this case, the apparent contact area could be determined using the equation: $A = \pi i g$, where i is the length of the semi-major axis and g is the length of the semi-minor axis (Figure 2 (a)). To calculate the

real contact area, the images of fingerprints were converted to binary black-white images, in which the non-contact region is presented as white and the real contact area refers to the inked area (Figure 2 (b)). The threshold of the image binarization was determined such that the boundaries of fingerprints before and after binarization were similar. The real contact area was calculated using the number of black pixels inside the outline of the contact zone in binary images.

<div align="center">(a)   (b)</div>
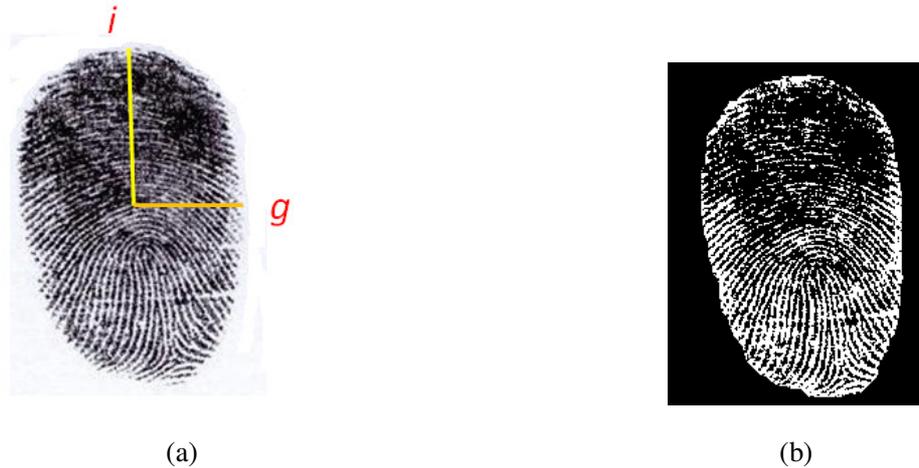
Figure 2: Images of a finger-pad ink print: (a) initial image where i and g are lengths of semi-major and semi-minor axes, respectively, (b) a binary image of (a) created in Matlab.

2.1.2 OCT Method

The Optical Coherence Tomography system (Michelson Diagnostic Ltd.) provides a new method to determine the real contact area. As shown in Figure 3 (a), a quartz glass window (Ra $\leq$ 0.01 mm) is inserted within a table, mounted on a force plate, built to allow finger-pad forces to be recorded while OCT images are collected. The set-up is similar to that described in previous studies [29-31]. 2D cross-section OCT images are generally used to study the sub-surface structure of the skin. In this study, the OCT system generates 2D images with a lateral dimension of 4 mm (x direction) and the penetration depth of (2 mm) (z direction). The resolution of images is about 15 µm (lateral) $\times$ 10 µm (axis). For the contacting area studies, a multi-slice OCT system was developed which is able to produce 16 slices. In the case of multi-slice scanning, the interval between slides in the y direction was set at 0.05 mm [31], which leads the scanning length in y direction to be $0.05 \times 16 = 0.8$ mm, hence the total scanning area (apparent contact area) could be estimated by A= $D_x \times D_y$ = 4×0.8 =3.2 mm^2 (see Figure 3 (b)). The real contact area was in accordance with the sum of lengths of flat regions in length. As it can be seen from the 2D image in Figure 3 (b), the top glass plate has strong light reflectance which result in difficulty in finding contacting and gap regions. In order to reduce the effect of light reflectance and improve the clarity of OCT images, the top surface of the glass plate was angled so as not to be perpendicular to the axis of the camera.

(a)	(b)
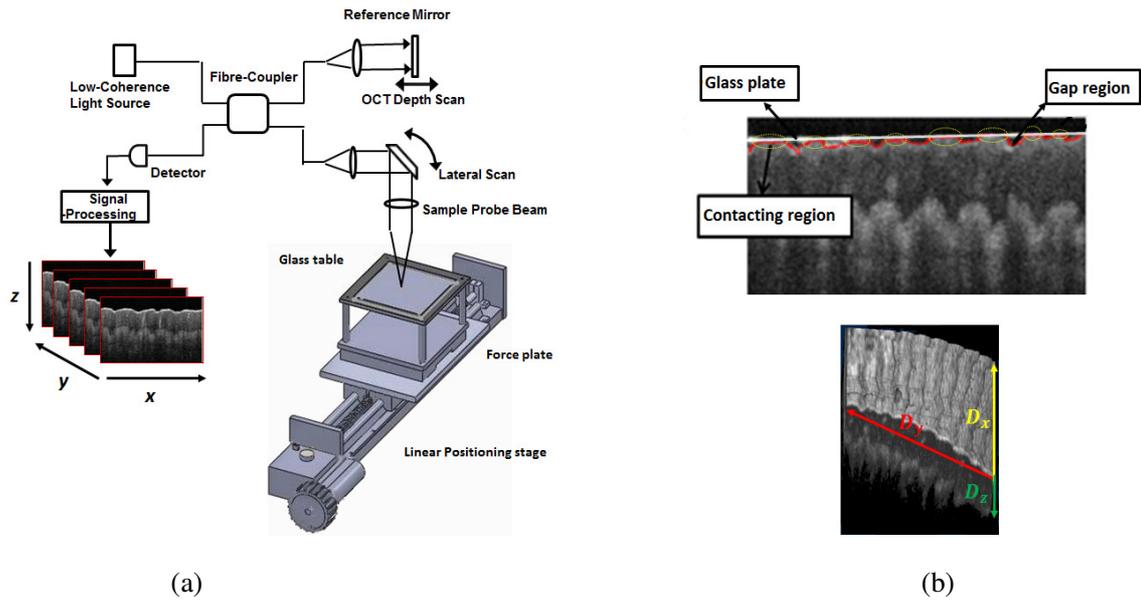
Figure 3: (a) schematic diagram of Optical Coherence Tomography system combined with a linear positioning stage and (b) an example of 2D and 3D image produced.

The experiments were carried out using the same finger as was used in the ink printing measurements. Due to the fact that the OCT system is limited to imaging a 4 ~ 6 mm wide rectangle of human skin, four different and representative regions of the finger-pad were selected to estimate the real contact area between the finger-pad and the contacting surface (see Figure 4). The participant was requested to wash her hands and dry them using a paper towel, prior to the test. The participant was then guided to press her index finger-pad against the glass window at various loads. The angle between the finger-pad and the glass window was controlled to be between 25° and 40°. During the process, the index finger was held stationary and not allowed to move away from the glass, which helped to ensure that the images of finger pad skin were scanned from the same position. In order to compare the OCT method with the ink printing method, the corresponding data with respect to the same tested positions on the finger-pad were also measured using the ink printing method.

(a)	(b)
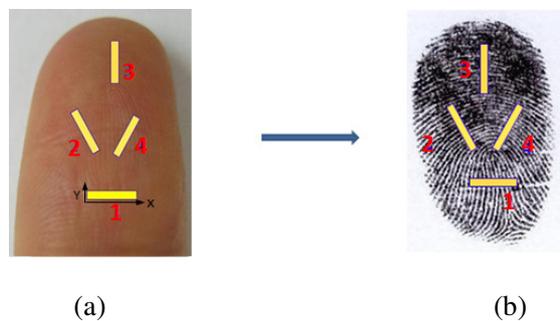
Figure 4: (a) Four different regions of the right index finger-pad were selected for comparing the OCT method, and (b) the ink printing method.

2.2 Measurements of Dynamic Contact Area

2.2.1   OCT Tests

In-vivo sliding experiments were conducted on the right middle finger of a 25 year old female (the same participant as used in the previous study) using the OCT system and the multi-axis force plate combined with a linear positioning stage (Reliance Precision Mechatronics), see Figure 3(a). The linear positioning stage included a carriage mounted with a multi-axis force plate on which a table with a glass window was attached. According to previous studies of human skin friction, most tests were performed at different speed conditions (range from 0.5 mm/s to 135 mm/s) [2, 32, 33]. In this study the speed of the linear positioning stages was set as 20 mm/s in order to simulate the movement of real finger. It is generally believed that the middle finger could give a relatively more precise control of stability when the finger is contacting with a sliding surface, compared to other fingers. Therefore, in the study of dynamic contact area the right middle finger was applied rather than the index finger. Measurements of dynamic contact were carried out by sliding the glass plate against the finger. During measurements, the subject was requested to hold the tested finger firmly against the glass plate and facing up towards the lens of the OCT system. The finger was required to stay in the same position and not allowed to move away from the glass plate throughout the entire test. Meantime both the normal and friction forces were also recorded by the multi-axis force plate, as well as the images of skin was scanned by the OCT. The set-up of the OCT system was very similar to that of the static contact area study. The frame rate of the OCT system was about 2.5 slices per second.

2.2.2   DIC Tests

A Digital Image Correlation system (DIC) was also employed to measure the dynamic contact area. The DIC is an optical technique which is generally used to measure deformation/strain of an object under load by tracking and matching the same points in two images recorded before and after deformation. As shown in Figure 5, the DIC system mainly consisted of a CCD (charge coupled device) camera, two lights and a computer. The experiments were carried out by the same participant, thereby using the middle finger of the right hand and the same apparatus used for the OCT measurements. The CCD camera was set to face down towards the glass plate which allowed it to capture the whole movement of the finger along the glass plate. The participant was instructed to initially slide her finger middle finger along the glass plate in a steady speed (approximately 10 -28 mm/s). The participant was then requested to carry out movements at various loads in the range of 2 to 25 N.

In this study, the tested finger was stained with a random pattern of black spots on its surface; the effect of the spots on friction measurements is considered to be relatively small and can therefore be neglected. Figure 6 (a) shows a reference image that was used for calibration (not in contact with the glass). The middle DIC image was recorded for the middle finger in contact with the glass window. It can be clearly seen that there is a relatively pale ellipse region on the finger-pad, which is considered as the contact region between the finger-pad and the glass window. The pale

region is due to reduced blood flow in capillaries within the finger-pad. In order to quantify the size of the pale region, the image is modified by enhancing the contrast. In the enhanced image, the contact area can be easily traced by a yellow line (Figure 6 (c)). The results of the contact area measured are in pixels, and therefore, they need to be converted to mm^2 (1 pixel = 2.5×10^{-3} mm^2).
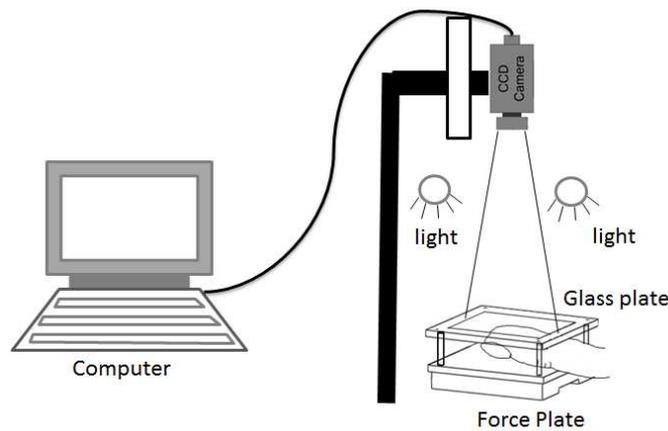
Figure 5: Schematic diagram of a Digital Image Correlation system.
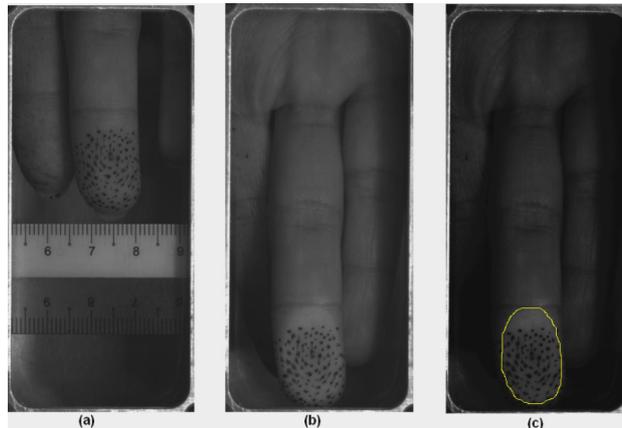
Figure 6: DIC images of the middle finger-pad: (a) a reference image, (b) an image for the finger pressing against the glass window and (c) an enhanced image of (b).

3. RESULTS AND DISCUSSION

3.1 Static Contact Area

3.1.1 The Effect of the Normal Load on the Contact Area

Figure 7 shows some images of fingerprints that were taken from the same index finger-pad under different loads. In this study, the apparent contact area of a finger-pad refers to the size of the fingerprint, and the real contact area depends on the amount of black ink. By comparing these

eight images, it can be found that the apparent contact area has an increasing trend with increasing load. These changes in the contact area (apparent and real) have been quantified and plotted in Figure 8. In order to study the effect of the normal load on the contact area in detail, these fingerprint images were divided into two groups considering the level of load applied, which is also believed to be helpful for explaining the two-part relationship of skin friction obtained.
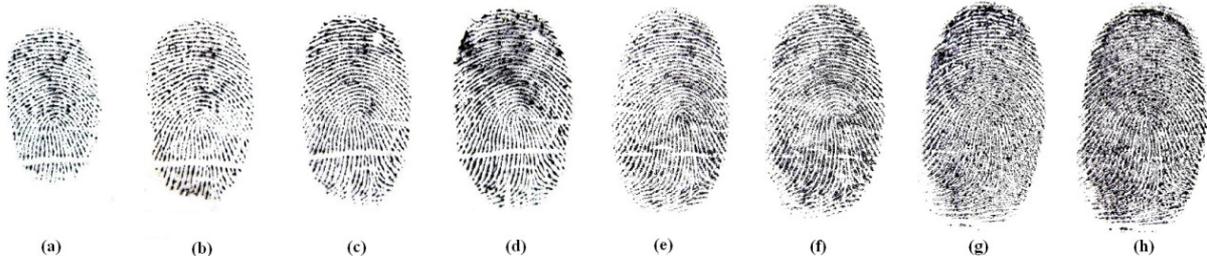
Figure 7: Binary images of fingerprints varying with loads, (a) 0.47 N, (b) 0.66 N, (c) 1.02 N, (d) 1.50 N, (e) 2.82 N, (f) 6.07 N, (g) 12.81 N and (h) 24.46 N.

Relationships between different contact parameters areas and the normal load were studied. In Figures 8 (a) and (b) the loads applied are split into two regimes above and below 2 N where a marked change in the area/load relationship was seen (note that this corresponds well with the change in friction/load behaviour seen by Tomlinson et al. [8]). With respect to the "low" load condition (< 2 N), as normal load increased, the results showed a 68% increase (from 78 mm^2 to 130 mm^2) in the apparent contact area and a 156% increase in the real contact area (from 16 mm^2 to 39 mm^2). The change in the apparent contact area at the "high" load condition is relatively smaller (a 30% increase) compared to that at the "low" load condition. As shown in Figure 8(b), the real contact area was also found to increase rapidly from around 40 mm^2 to 94 mm^2. The increasing trends for all contact areas were found to obey the following expression:

$$A = \begin{cases} aN^m & at\ low\ load\ condition \\ bN^n & at\ high\ load\ condition \end{cases} \tag{1}$$

where N is the normal load, a, b are constant and m, n are the exponent of N (constant). As suggested by the equation, the apparent contact area is dependent on the normal load to the power 0.42 (at the "low" load condition) and 0.14 (at the "high" load condition), the parameters a and b were calculated to be 107 and 130 respectively. The corresponding exponents for real contact area were found to be 0.50 (at the "low" load condition) and 0.28 (at the "high" load condition), where a=27 and b=31. A similar piecewise linear correlation was also introduced for the real contact pressure (calculated by dividing normal loads by real contact areas) and the normal load.

$$P = \begin{cases} kN^j & at\ low\ load\ condition \\ tN^h & at\ high\ load\ condition \end{cases} \tag{2}$$

where k, t are constant and j, h are the exponent of N (constant). Best-fit curves to Equation (2) for the data set is given in Figure 8 (c), the parameter values for the data set are: $k = 38, j = 0.56$, $t = 34$ and $h = 0.70$. The linear correlation coefficient $p = 0.97$ and the coefficient of determination $R^2=0.93$.

Human skin is a heterogeneous, anisotropic and a non-linear viscoelastic material [34, 35]. Owing to these properties, skin allows more material to come into direct contact with a surface and hence the contact areas increases with increasing load. Figure 8 (a) shows that the apparent contact area has a rapid increase at the low load condition and it reaches a plateau (at approximately 200 mm^2) at the high load condition. This observation could be explained by the stress-strain behaviour of the skin [35-38]. In the case that low magnitude loads are applied to human skin (phase II), the collagen fibres in the skin will be straightened, and result in large deformations, which is reflected on the steep increase of the apparent contact area. When the external load goes beyond a certain level, the stress-strain relationship tends to be linear due to the fact that skin gradually approaches its maximum extension, becomes stiff, which leads to smaller and smaller deformations being possible (phase III). Therefore, there was no significant change observed in the apparent contact at the high load condition. The real contact areas obtained in both cases show different change of trend line compared to those of the apparent contact areas. Due to the fact that the real contact area is related to the junctions of the skin asperities and a surface, it will keep increasing because of the deformation of asperities on the skin surface, though the apparent contact area no longer changes.
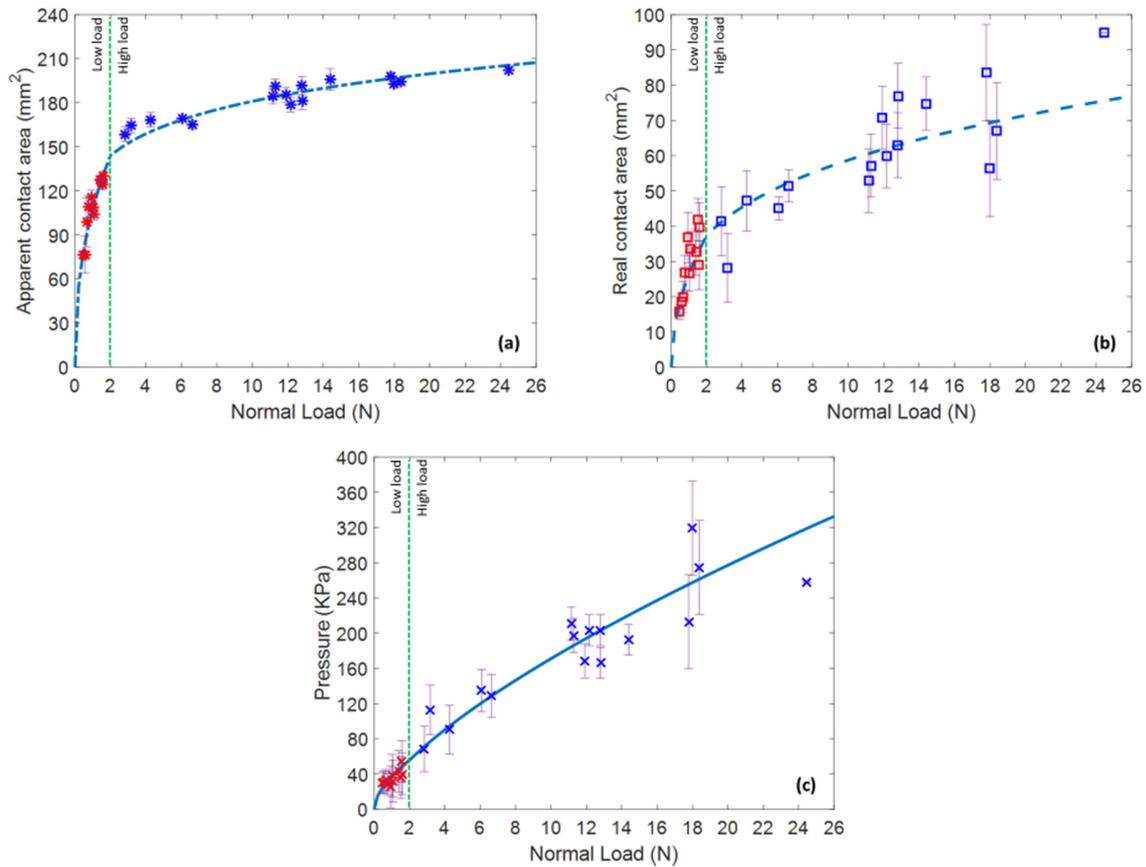
Figure 8: The contact area and the pressure obtained for a finger-pad in contact with paper sheets in the present study with model fits: (a) apparent contact area: experimental data (star) (mean values ± SD) and model fit (dash dot line). (b) real contact area: experimental data (square) (mean values ± SD) and model fit (dotted line). (c) real contact pressure: experimental data (cross) (mean values ± SD) and model fit (solid line).
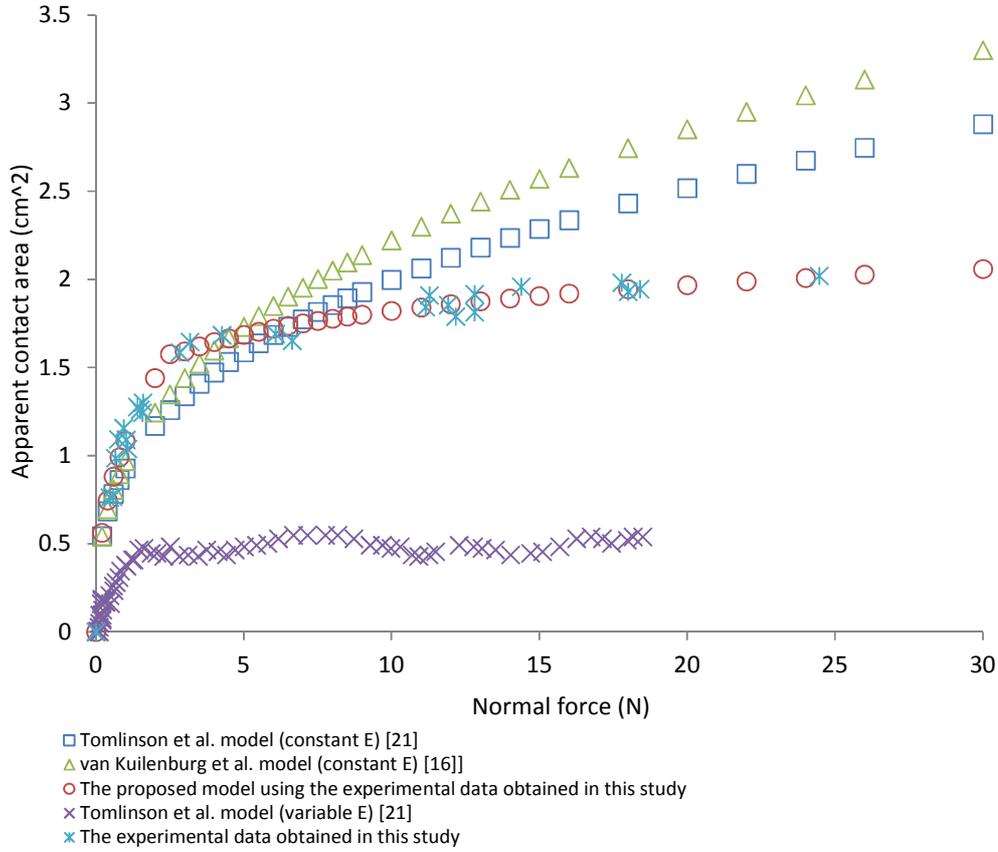
Figure 9: Variation of the relationships between the apparent contact area and the normal load for different methods.

As suggested by Hertz, the contact area for non-linear elastic materials would be expected to increase with the normal load to the power of 2/3, and is given by the expression:

$$A = \pi \left(\frac{9NR}{16E}\right)^{2/3} \tag{3}$$

where R is the radius of the sphere and E is the reduced Young's modulus [25]. In general, it is believed that human skin exhibits similar mechanical properties to those of the rubber. Therefore, the Hertz theory has been widely used to estimate the contact mechanism of human skin. For example, Tomlinson [21] modified the Hertz contact model in order to determine the contact area between human fingers and a flat surface. With respect to her new model, R was assumed to be the radius of the finger, E was the reduced Young's modulus $= \frac{(1 - v_{skin}{}^2)}{E_{skin}}$, E_{skin} is the Young's modulus of human skin (approximately 0.49 MPa) and v_{skin} is the Poisson's ratio of human skin (approximately 0.5). A similar model was also proposed by van Kuilenburg et al. [16], they found that the apparent contact area depends on the normal load to the power of 0.36. In this study, a comparison between the estimated contact areas calculated using different Hertz models and the experimental data obtained in this study has been made (see Figure 9). In the case

12

of constant Young's modulus, it can be seen that the results of Tomlinson and van Kuilenburg show a similar linear behaviour. The values of the exponent for the current experimental data range from 0.11 to 0.41 which is in a good agreement with the experimental results of Han et al. [11]. They have investigated the contact area between human fingers and a transparent acrylic board using a CCD camera and found that the corresponding exponent value ranged from 0.2 to 0.4. They reasoned the Hertzian contact theory is not suitable to calculate the contact area as human fingers do not experience spherical point contact. This assumption was evidenced by Figure 6 in the current study. In the study of Xydas & Kao [39], they found that the corresponding exponent values of their experiments were found to be 0.55 for rubber fingers, 0.51 for silicone fingers and 0.09 for real fingers. Moreover, they indicated that the Hertz model is a linear elastic model and since human skin exhibits as a non-linear elastic material involving large deformations, the Hertz model with constant Young's modulus could not be used to describe the contact mechanism of human fingers. A similar conclusion was also drawn by Tomlinson [21], they found that the area of contact calculated using vary Young's modulus and their experimental data show similar change trend with some minor difference.

In the recent study carried out by Derler et al. [7], who looked at the effect of the normal load on the apparent contact areas for both the edge of hand and a finger using a CCD camera. The experimental data points for each anatomical site were fitted into a polynomial equation: $(N) = B + U.N^{1/4} + H.N$, where B, U, and H were constant. They found that there are steep initial increases on the apparent contact area with load for both anatomical sites (between 1 N and 4 N). When the applied load increased above 10 N, the apparent contact area reached a plateau with maximum value of about 4 cm^2 on the index finger and 15 cm^2 on the edge of the hand, respectively. Though they applied a polynomial model to describe the relationship between the apparent contact area and the normal load, rather than a power-law model, their trends of changes are consistent with the results of Tomlinson. [21] and van Kuilenburg et al. [16]. Their model is very accurate based on the experimental data, however, the polynomial expression is not consistent with the general understanding about human skin friction. In principle, the contact area should be zero when no load applied on the finger-pad, but the suggested model does not agree with it.

The analysis of the results shown in Figure 8 indicated that the contact areas between the human finger-pad and paper sheets follow a piecewise linear function. It can also be observed that this proposed model presented excellent fitting capabilities with p=0.99 and R^2=0.98 for the apparent contact area, p=0.93and R^2=0.85 for the real contact area. Soneda and Nakano [22] have conducted a similar study of contact area using the optical method. They found that both the apparent and real contact areas increased following the power law $A \propto N^c$ when the load increased. The dependence of the apparent contact area (A_o) was 0.52 ± 0.06 and the real contact area (A_{re}) was 0.68 ± 0.09 for load between 0.1 N and 5 N. A similar observation was also reported by Warman and Ennos [20], who indicated that the apparent contact area rose with the normal load to power between 0.54 and 0.85 for all five fingers under the condition of a load less

than 2 N and the real contact area was about 66.7% of the total perimeter area. These results appear large in contrast with the results of this study. In this study, under the low load condition, the corresponding exponent of A_o was 0.42 and the exponent of A_{re} was 0.50. Increasing the normal force, the exponent of A_o reduced to 0.14 and 0.28 for the exponent of A_{re}. These wide variation ranges in the exponents for both A_o and A_{re} among the above studies could be attributed to several possibilities. The first possibility is that the results in the experiments of the ink printing method were inaccurate due to these drawbacks of ink spread, noise effect, threshold setting, etc. The second possibility may lie in the difference among the various tested subjects and finger-pads. Environmental conditions, such as temperature and humidity, test materials, and performing angle will also influence the results. In summary, it is reasonable to conclude that the proposed piecewise model is a reliable model describe and accurately predicts the contact area between the human finger-pad and a smooth surface with respect to various loads applied in dry conditions.

3.1.2   OCT Tests

Considering the disadvantages apparent in the research using ink printing method, it was hard to obtain accurate results of both apparent and real contact areas, particularly the real contact area. Thus, a new method of measuring real contact area was explored. The OCT image method was used to measure the contact area based on the technique of producing cross-section area image of skin.

The normal force used in both the OCT method and the ink printing method ranged from 0.1 N and 2.5 N, thus this could be considered as a low load condition. For that, the relationship between the real contact area and the normal load could be described using Equation (1), with the coefficient of determination (R^2): $A_{re} = a_{re}N^{m_{re}}$, where a_{re} is constant, m_{re} is the exponent of N (constant). Figure 10 displays the experimental results that were measured in four different positions on the examined finger-pad, in which, with increasing normal load, the real contact area was found to increase by approximately 20% for the OCT method, and 10% for the ink printing method.

Table 1 shows some parameters of the power-law relationship between the real contact area to the normal load obtained from both methods. The exponent m_{re} was found to range from 0.12 to 0.20 for the OCT method and from 0.40 to 0.66 for the ink printing method depending on different positions (see Figure 4). With respect to the coefficient of determination, the OCT method presents a high correlation between the real against the normal load due to the values of (p) varying between 0.004 and 0.1 for all different positions. In contrast to the OCT method, the corresponding values of (p) obtained from the ink printing method are generally much larger (≥ 0.05) than those OCT results, thus the correlation between these two variables is not significant.
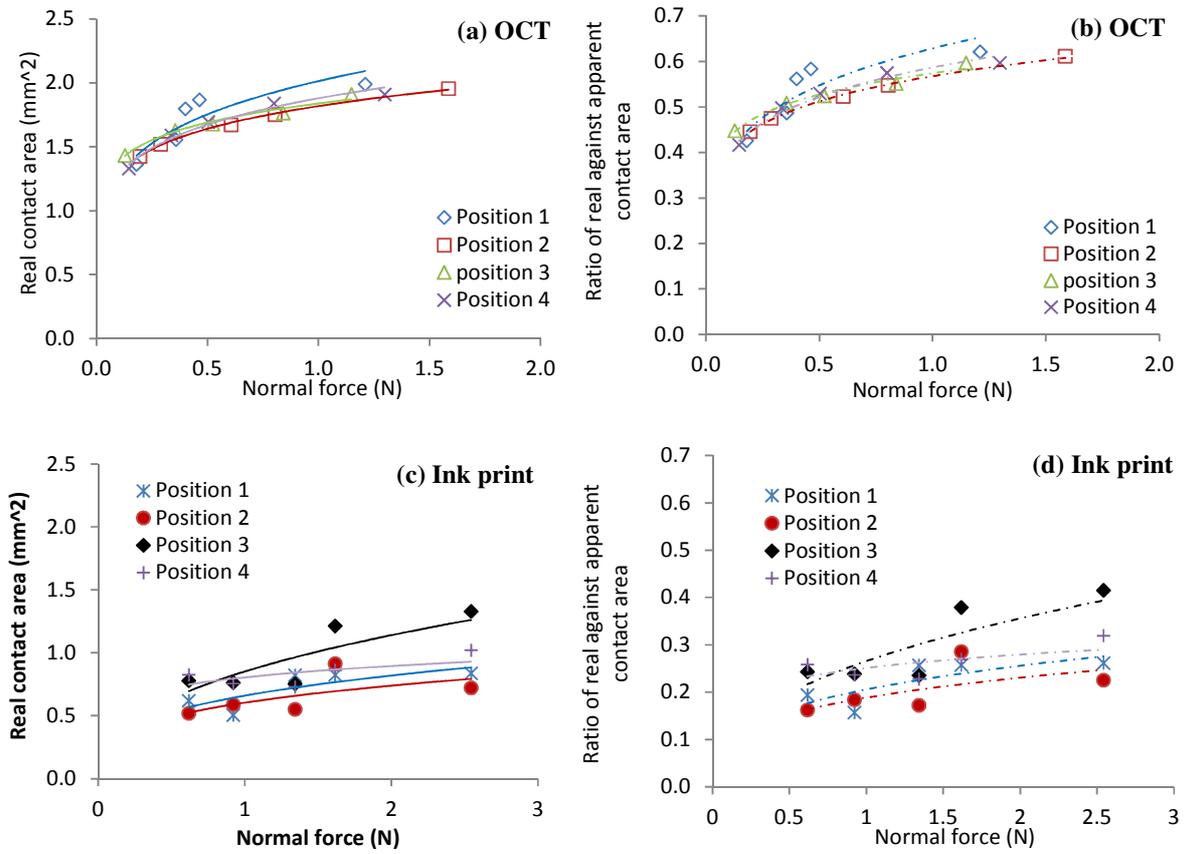
Figure 10: Real contact area as a function of the normal load for four different positions: (a) OCT method and (c) ink printing method. The corresponding data of the ratio of the real contact area against the apparent contact area with load: (b) OCT method and (d) ink printing method.

Table 1: Some parameters of the power-law relationships between the real contact area as a function of the normal load obtained from both methods.

position	OCT method				ink printing method			
	constant (a_{re})	exponent (m_{re})	p	R^2	constant (a_{re})	exponent (m_{re})	p	R^2
position 1	2.01	0.20	0.114	0.80	0.21	0.31	0.153	0.56
position 2	1.82	0.15	0.004	0.99	0.19	0.29	0.310	0.46
position 3	1.84	0.12	0.004	0.98	0.27	0.42	0.054	0.66
position 4	1.88	0.17	0.033	0.98	0.25	0.15	0.111	0.40

Note: p is correlation and R^2 is the coefficient of determination.

As mentioned previously, there have been several previous studies using the ink printing method. Tomlinson [21] reported that the contact area of the examined finger increased with load

following a linear relationship, and the ratio of the ridges area to the total area was between 0.38 and 0.5. In the similar studies of Childs & Henson's [19], the apparent contact area increased with load (up to 2 N). The percentage of the real contact area to the apparent contact area was found to increase with load as well. The ratio was 12% at the load of 0.41 N, increased to 34% when the load rose to 1.77 N. These results are very similar to the results in the current study. As can be seen in Figure 10 (d), the results of the ratio were fitted into a curve regression. The percentages of the real contact area to the apparent contact area were found to be around 0.15 for 0.5 N, and 0.3 for 2 N. These results were also in good agreement with the experimental results from the experiments of Soneda & Nakano [22], who developed a device based on light reflection for investigating the contact mechanism of human fingers. The principle of the measurements of the apparent contact area and the real contact area relates the morphology of the finger skin. They found that the mean value of $\frac{A_{re}}{A_o}$ was 0.3 at a contact of 1 N.

However, in contrast to the above results, the OCT method shows a relatively higher percentage, about 0.45 for 0.2 N and 0.60 for 1.2 N (see Figure 10 (b)). This difference could be attributed to several factors. The first possibility is that the real contact length measured between finger skin and the glass plate was over-estimated. In the OCT tests, the measurement of the real contact area was done by manual observation. Due to the fact that there was strong light reflectance from the glass plate and the superficial of the stratum corneum it was not always straightforward to determine the bounds of ridge contact which can result in that some gap regions between the glass plate and skin ridges was accounted as contacting regions, and hence cause high ratio of real to apparent contact area. The second possibility could be attributed to the effect of ink spread, noise effects and threshold value setting in measurement of contacting areas using ink printing method. It can be assumed that the area of ink coverage would increase due to ink spread, and can result in a large apparent contact area. Inappropriate choice of threshold value setting in image processing can cause some amount of ink coverage might be lost, hence a small real contact area.

Furthermore, it can be seen that the experimental results of OCT method show the linear regression models with respect to four different positions have greater similarities than those in the ink printing test data. Additionally, it was noted that the correlation (*p*) related to these linear regression models obtained are ranged from 0.004 to 0.114 for the OCT tests, 0.054 to 0.310 for those ink printing tests. These strong correlation relationships between variables in Table 1 reveal that the OCT method provides more reliable experimental results than use of the ink printing method. Though the OCT technique is restricted to measurement of small regions in finger-pads, it provides a suitable method for examining the internal micro-structure of skin that could help to predict the changing trends in the real contact area of finger-pads. The issues with the OCT image analysis can be overcome by developing a suitable algorithm to assess the bounds more accurately than can be done by eye.

3.2 Dynamic Contact Areas

3.2.1   OCT Tests

Figure 11 shows two OCT images of the finger in contact with the glass under static and sliding contact conditions. During the preloading phase (static phase), the finger ridges came into contact with the glass surface, as shown in Figure 11 (a). It can be seen that the skin does not completely contact with the glass plate as some gaps were found between the skin and the glass plate. As the glass plate began to move against the finger-pad, a friction force arose from the relative motion that deformed the ridges and increased the contact area (see Figure 11 (b)). Unfortunately, these changes in the contact region were not easy to quantify reliably.
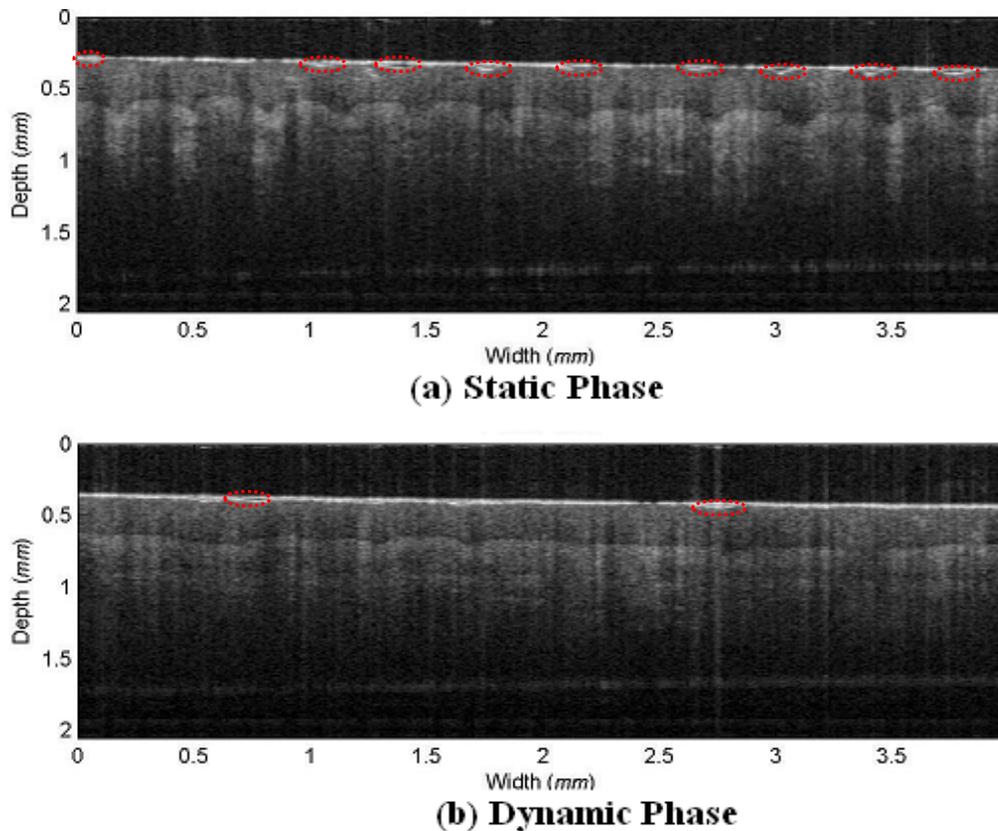

Figure 11: OCT images of finger skin in contact with the glass (gap between the skin and the glass plate was marked by red circle), which were obtained from (a) static phase and (b) dynamic phase.

3.2.2   DIC Tests

Figure 12 shows a schematic diagram of a finger moving along a glass plate. DIC images of the tested finger-pad were collected at different positions. Figure 13 displays the corresponding plot of the friction force and the normal force obtained from the multi-axis force plate during finger sliding, as well as some correlated DIC images of the finger-pad. In these DIC images, the direction of finger movement across the glass window is shown by a green arrow. Meanwhile,

the contact regions on the finger-pads were also traced by dashed lines with respect to different stages of movement.
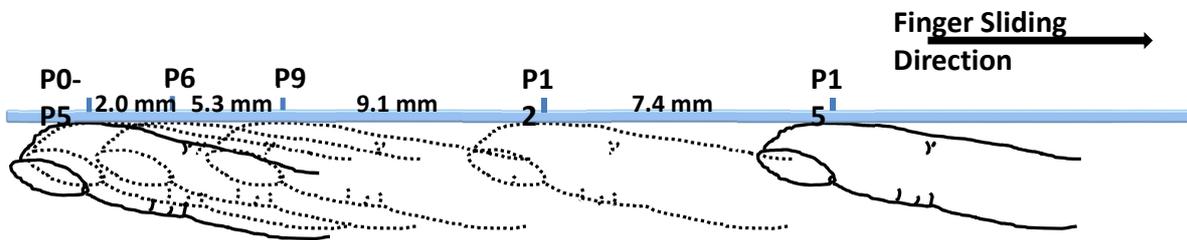
**Figure12:** Schematic showing points at which DIC images of a finger-pad (from P0 to P15) were taken when moving along a glass plate: P0-P5 were collected from the pre-movement period, P6 was taken from the point that the finger started to move, and P9-P15 were taken during the movement period.
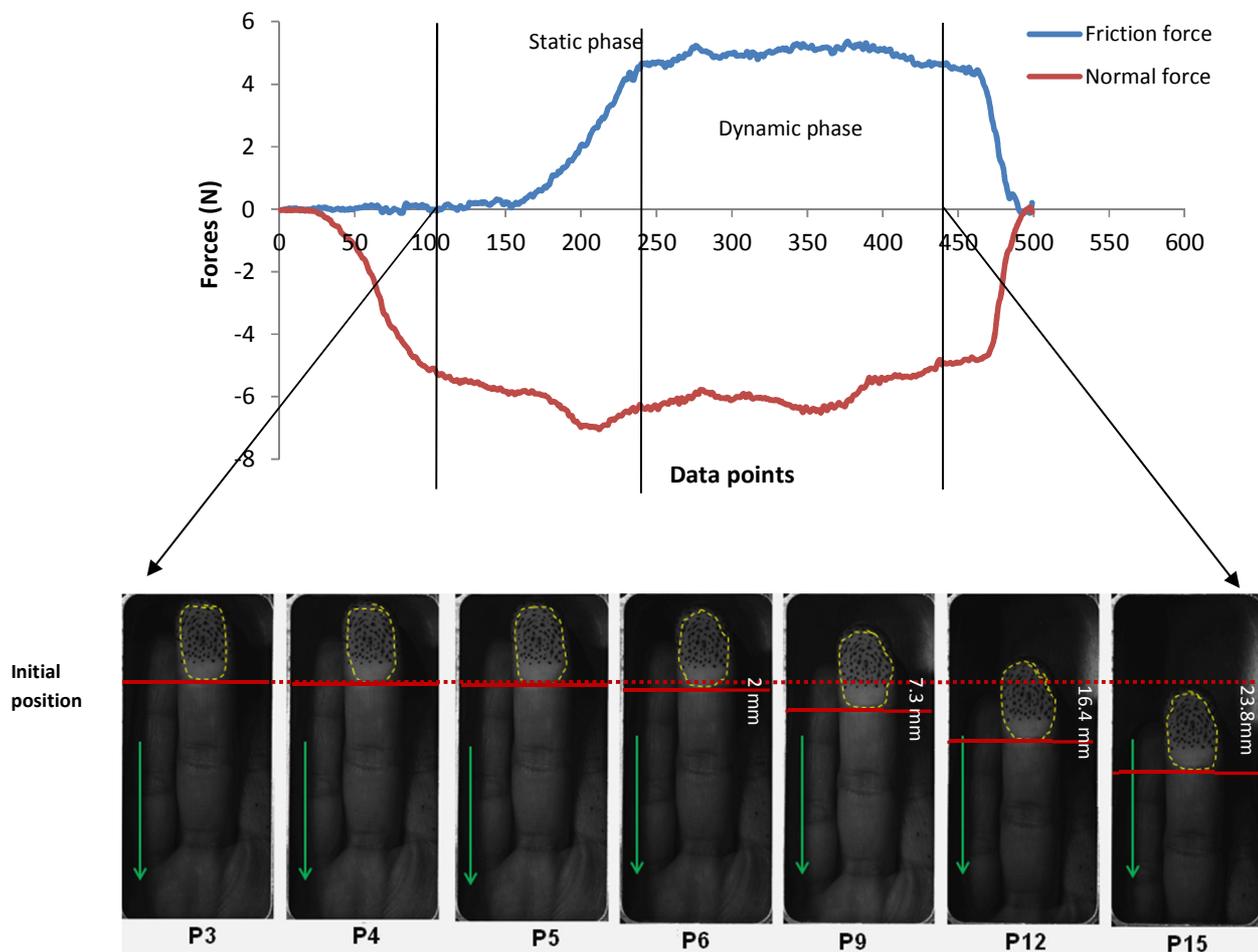
Figure13: Friction force and normal force, along with the corresponding finger-pad images from the DIC system.

These experimental results and images were divided into a static phase (adhesion) and a dynamic (slip) phase (Figures 14). Each phase has been assessed individually. Figure 14 (a) shows the experimental results of the apparent contact area as a function of time for the finger sliding over the glass window at a constant normal force 6 ± 0.5 N. In the static phase, the contact area is found to decrease from 230 mm^2 to 214 mm^2. However, there was no significant change observed in the contact area with time in the dynamic phase. Figure 14 (b) shows the time-dependent evolution of the friction force during the same period of Figure 14 (a). The friction force was found to gradually increase before sliding began at around 4.9 s. After that, the finger started to slip with a constant friction force of about 4.8 ± 0.2 N.
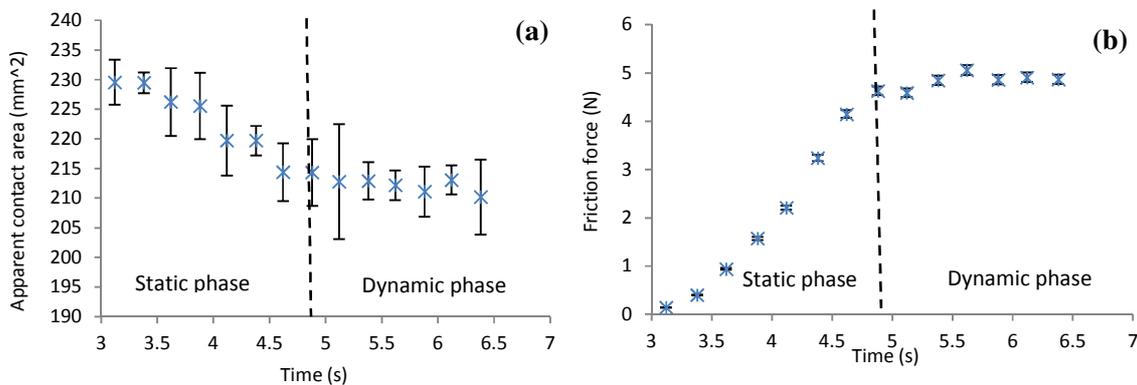
Figure 14: (a) The apparent contact area as a function of time for a middle finger sliding along a glass window (mean values ± SD). (b) The friction force as a function of time for an middle finger sliding along a glass window (mean values ± SD).

André et al. [27] conducted some experiments to investigate the contact mechanism of human fingers in contact with a smooth glass surface during the transition from the stuck contact to full slip, under dry and wet conditions. These experiments were performed using an optical fingerprint recording system combined with a force sensor, in which the areas of contact regions on finger-pads were present as ellipses. The experimental results showed that the normalized contact area between the examined fingertip and the prism varies with subjects. As the normal load was increased from 0.2 N to 10 N, the normalized contact area was increased by a factor of three. They also found that there is 12.5% decrease in the horizontal ellipse axis with time at a constant normal force of 5 N, which revealed that the normalized contact area was decreased by 6.25. They suggested that the decrease in the normalized contact area during preloading may be due to the initial deformation of skin. These observations are in good agreement with the results of our studies. Figure 14 (a) shows that the apparent contact area has a decrease of 7% when the middle finger moves along the glass window during the transition from the static phase to the dynamic phase. The corresponding friction force was found to increase instead which could be attributed to the increase of real contact area, hence increase the adhesion force. This assumption is also validated by the above OCT studies. As it can be seen in Figure 11, the gap regions between the finger-pad and the glass window are diminished when the finger transfers from the

static phase to the dynamic phase, and leads more skin in contact with the glass plate. Owing to the increase in the friction force, the skin on the surface of finger-pads was stretched in the same direction of finger movement (lateral direction), which results in a decrease in the dimension of the contact region in the horizontal direction. However, no significant change occurred in the lateral dimension of the contact regions.

From previous studies, it is noted that the friction of skin is assumed to be only associated with an adhesion mechanism in the case of fingers in contact with dry and smooth surfaces, while the deformation is normally ignored [4-6]. The friction force is generally reported to be proportional to the real contact area. Therefore, we can assume that as the real contact area of a finger-pad decreases, the friction force will decrease. However, in this study, the experimental results obtained are the apparent area of contact between human finger-pads and surfaces, which could not be used to estimate the friction force based on the above theory. Terekhov & Hayward [40] have developed a simple numerical model to characterise the friction force between a fingertip and a flat surface in the stick-slip transition. This model is given by:

$$F = \pi i g r_s{}^2 q_{stick} + \mu N (1 - r_s{}^2)^2 \tag{4}$$

where $r_s{}^2$ is the stick ratio of the stuck area to the total contact area which varies from 1 (unloaded contact) to 0 (fully slipping contact); μ is the dynamic friction coefficient; and q_{stick} is the traction $q(x, y)$ in the stuck region [16, 27]. In the case that the support boundary condition is assumed to be far from the contact region between skin and surfaces, the traction is assumed to be uniformly distributed in the contact region and is given by:

$$q(x, y) = \begin{cases} q_{stick} & in\ stuck\ region \\ \mu p(x, y) & in\ slip\ region \end{cases} \tag{5}$$

where $p(x, y)$ is the pressure distribution with the contact region. At the adhesion condition, q_{stick} can be expressed as:

$$q_{stick} = \left(\frac{2\mu_s N}{\pi i g}\right)(1 - r_s{}^2) \tag{6}$$

where μ_s is the static friction coefficient. By adding Equation (6) to Equation (4), the model could be simplified as:

$$F = 2\mu_s N(1 - r_s{}^2)r_s{}^2 + \mu N(1 - r_s{}^2)^2 \tag{7}$$

From Figure 14, it can be seen that the maximum value of the static friction force is similar to the average dynamic friction force at a constant normal load of 6 N. Therefore, it can be assumed that the static friction coefficient (μ_s) is the same as the dynamic friction coefficient (μ) in the case of fingers in contact with dry and smooth glass surfaces. Therefore, Equation (7) can be expressed as:

$$F = \mu N[2(1 - r_s{}^2)r_s{}^2 + (1 - r_s{}^2)^2] \tag{8}$$

That is, the friction force is strongly dependent on the stick ratio ($r_s{}^2$) due to the dynamic friction coefficient and the normal load are constant. Terekhov & Hayward [40] indicated that the stuck contact area reduces with increasing friction force. However, this conclusion is only valid if the dynamic friction coefficient is larger than the static friction coefficient. For the case that the dynamic friction coefficient is equal or smaller than the static friction coefficient, no related discussion was given in their study. A similar conclusion was also drawn by André et al. [27], they found that both the stick area and the total contact area decrease over time when fingers sliding along a flat surface. As the friction force increased, the stick area had a significant decrease compared to the total contact area, hence the stick ratio was shown to gradually decrease from 1 to 0. On the basis of above findings, it could suggest that the stick ratio of the stuck area to the total contact area decreases in the transition from a stuck state to full slip, and results in an increase in the friction force.
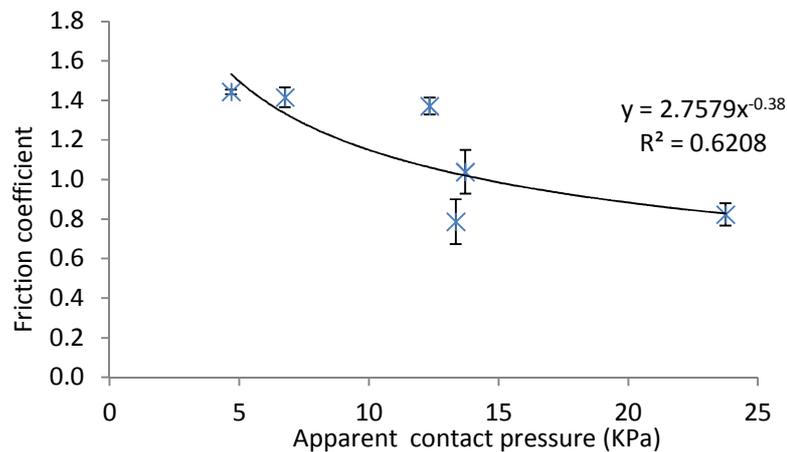
Figure 16: Dynamic friction coefficient measured as a function of the contact pressure applied (mean values ± SD).

From the above findings, it has been shown that the apparent contact area and the friction force vary with time in the static phase, and both of them reach steady-state in the dynamic phase. In this section, in order to gain accurate results of the contact areas and the friction coefficients, at least two DIC images with related friction data obtained from a point in the steady-state phase were analysed. Figure 16 shows the skin friction coefficient plotted as a function of the apparent contact pressure. These experimental data points can be fitted by a curve and described by a power-law model with the exponent of -0.38, as expected. The coefficient of determination (R^2) was around 0.62. Furthermore, the skin friction coefficient was found to decrease by 42% when the apparent contact pressure increased from 4.7 kPa to 23.8 kPa.

In order to investigate the effect of the contact pressure on skin friction, Adams et al. [6] derived an expression based on the adhesion mechanism dominating the skin friction in the case that skin is in contact with a smooth glass surface under dry conditions. This simple model is given as:

$$\mu = \frac{F}{N} = \frac{\tau_0 A_{re}}{N} + \alpha \qquad (9)$$

where τ_0 is the intrinsic interfacial shear strength ($\tau = \tau_0 + f\frac{N}{A_{re}}$), and f is a pressure coefficient. Figure 8 (b) suggest that the real contact area between human fingers and flat surfaces can be written as:

$$A_{re} = \begin{cases} a_{re}N^{m_{re}} & \text{at low load condition} \\ b_{re}N^{n_{re}} & \text{at high load condition} \end{cases} \qquad (10)$$

where a_{re} and b_{re} are constant, m_{re} and n_{re} are the exponent of N (constant). Adding it to Equation (9), we obtain:

$$\mu = \begin{cases} (\frac{\tau_0 a_{re}N^{m_{re}}}{N} + f) \propto N^{m_{re}-1} & \text{at low load condition} \\ (\frac{\tau_0 b_{re}N^{n_{re}}}{N} + f) \propto N^{n_{re}-1} & \text{at high load condition} \end{cases} \qquad (11)$$

The real contact pressure was found to increase with the normal load following a piecewise linear model (see Equation (2)), and is given as:

$$P = \begin{cases} kN^j & \text{at low load condition} \\ tN^h & \text{at high load condition} \end{cases} \qquad (12)$$

Therefore, the relationship between the skin friction coefficient and the real contact pressure could be described as follows:

$$\mu \propto \begin{cases} P^{(\frac{m_{re}-1}{j})} & \text{at low load condition} \\ P^{(\frac{n_{re}-1}{h})} & \text{at high load condition} \end{cases} \qquad (13)$$

According to the results in Figure 8, the exponent m_{re} related to the real contact area is found to be 0.50 at load between 0.4 N and 1.8 N, and n_{re} is 0.28 at load between 3 N and 24 N. The value of the exponent $j = 0.56$, $h = 0.70$. The exponent of P in Equation (13) is calculated to be -0.9 at the low load condition, and -1 at the high load condition. Soneda & Nakano [22] used a model $\mu \propto P^{-(\frac{1-n_{ap}}{1-n_{re}})}$ (where n_{ap} is the exponent related to the static area of apparent contact and n_{re} is the exponent related to the static area of real contact) to analyse the relationship between the skin friction coefficient and the contact pressure. For loads range between 0.1 N and 10 N, the exponent of P was calculated to be -0.67. A study was also carried out by Derler et al. [7], in which subjects rubbed their index fingers and the edges of hands against smooth glass and rough glass with loads up to 50 N, under dry and wet conditions. They found that the skin friction coefficients for both anatomical sites decrease with increasing the contact pressure in accordance with the model of: $\mu \propto P^Q$. The exponent Q was found to be ranged from -0.79 to -0.96 for the case that dry fingers were dragged along a smooth glass. The corresponding value of exponent Q

was between -1.05 and -1.42 under wet sliding conditions. It is interesting to note that these results related to dry sliding condition are close to these calculated results in this section. Additionally, it can be seen that Derler's model [7] is slightly different from the model in the current study, because it was assumed that the contact pressure is independent of the normal load. However, in this study, it is shown that the contact pressure is strongly associated with the normal force in a relationship represented by a two-term function rather than a linear function (Figure 8 (c)).

Compared to the results measured directly from the DIC tests, the value of the exponent P obtained from Equation (13) is relatively large. This observation could be explained by the fact that the values of these parameters used in Equation (13) were derived from the measurements of static contact areas, which are different from those in the DIC tests. As suggested by Figure 14 (a), the dynamic areas of apparent contact are always smaller than the static areas of apparent contact. A similar phenomenon should be expected in the real contact area. These differences in the real contact area between the static and dynamic movements contribute to different values for the exponents (i.e., m_{re}, n_{re}, j and h), thus result in different exponents of p.

4. CONCLUSIONS

In this paper, the contact area between human finger-pads and flat surfaces was investigated using different techniques. In the static measurements, the contact area was found to be dependent on the normal load. At the low load condition (< 2 N), there was a rapid increase in both the apparent and the real contact area, the corresponding changes in both contact areas were relatively small at the high load condition, especially the apparent contact area. This could be attributed to the viscoelastic properties of the human skin. A piecewise linear model was proposed to estimate the effect of load on the apparent contact area and the real contact area under low load and high load conditions.

This study also assessed the dynamic changes in contact area using the OCT technique and the DIC technique. Experimental results of the DIC method showed that the dynamic apparent contact area reduces with time in the transition from the static phase to the dynamic phase. The apparent pressure dependence of skin friction coefficient was in accordance with a piecewise linear function with an exponent of -0.9 and -1 with respect to different load conditions. Though, the OCT technique could not provide actual data of contact areas for both the static and the dynamic measurements, it would be very useful for understanding the skin surface topographical properties of the human finger-pads due to friction on the micro-scale level.

REFERENCES

1. Derler, S., Gerhardt, L.-C., "Tribology of skin: review and analysis of experimental results for the friction coefficient of human skin", Tribology Letters; 45: 1-27, 2012.
2. Tomlinson, S. E., Lewis, R., Carré, M. J., "Review of the frictional properties of the finger-object contact when gripping", Journal of Engineering Tribology, Proceedings of the IMechE Part J; 221: 841-850, 2007.
3. Bowden, F. P. and Tabor, D., The Friction and Lubrication of Solids. Oxford University Press, London, 219-221, 1964.
4. Wolfram, L. J., "Friction of skin", Journal of the Society of Cosmetic Chemists; 34: 465-476, 1983.
5. Johnson, S. A., Gorman, D. M., Adams, M. J. and Briscoe, B. J., "The friction and lubrication of human stratum corneum", In: Thin films in tribology. Leeds–Lyon symposium on tribology, Amsterdam: Elsevier Science Publishers; 663–72, 1993.
6. Adams, M., Briscoe, B., Johnson, S., "Friction and lubrication of human skin", Tribology Letters; 26(3): 239-253, 2007.
7. Derler, S., Gerhardt, L. C., Lenz, A., Bertaux, E. and Hada, M., "Friction of human skin against smooth and rough glass as a function of the contact pressure", Tribology International; 42: 1565–1574, 2009.
8. Tomlinson, S. E., Lewis, R. and Carré, M. J., "The effect of normal force and roughness on friction in human finger contact", Wear; 267: 1311-1318, 2009.
9. Lodén, M., Olsson, H., AxeÂll, T. and Werner, L. Y., "Friction, capacitance and transepidermal water loss (TEWL) in dry atopic and normal skin", British Journal of Dermatology; 126: 137-41, 1992.
10. Gulati, R. J. and Srinivasan, M. A., "Human fingerpad under indentation I: static and dynamic force reponse", Bioegineering Conference; 29, 1995.
11. Han, H. Y., Shimada, A. and Kawamura, S., "Analysis of friction on human fingers and design of artificial fingers", International conference on robotics and automation; 3061-3066, 1996.
12. Sivamani, R. K., Goodman, J., Gitis, N. V., Maibach, H. I., "Coefficient of friction: tribological studies in man – an overview", Skin Research and Technology; 9: 227 – 234, 2003.
13. van der Heide, E., Zeng, X. and Masen, M. A., "Skin tribology: Science friction?", Friction; 1: 130-142, 2013.
14. Persson, B. N. J., Kovalev, A., Gorb, S. N., "Contact mechanics and friction on dry and wet human skin", Tribology Letters; 50, 17–30, 2013.
15. Lewis, R., Carre, M. J., Tomlinson, S. E., "Skin friction at the interface between hands and sports equipment. Procedia Engineering", 72: 611-617, 2014.
16. van Kuilenburg, J., Masen, M. A. and van der Heide, E., "The role of the skin microrelief in the contact behaviour of human skin: Contact between the human finger and regular surface textures", Tribology International; 65: 81-90, 2012.

17. van Kuilenburg, J., Masen, M. A, van der Heide, E., "A review of fingerpad contact mechanics and friction and how this affects tactile perception", Proceedings of the IMechE Part J. Journal of Engineering Tribology; 229 (3), 243-258, 2015.

18. Derler, S., Preiswerk, M., Rotaru, G. M., Kaiserb, J. P., Rossia, R. M., "Friction mechanisms and abrasion of the human finger pad in contact with rough surfaces", Tribology International; 89, 119–127, 2015.

19. Childs, T. H. C. and Henson, B., "Human tactile perception of screen printed surfaces: self-report and contact mechanics experiments", Proceedings of the IMechE Part J. Journal of Engineering Tribology; 427-441, 2006.

20. Warman, P. W. and Ennos, A. R., "Fingerprints are unlikely to increase the friction of primate fingerpads", Journal of Experimental Biology; 212: 2015-2021, 2009.

21. Tomlinson, S. E., Understanding the friction between human finger and contacting surfaces, PhD Thesis, The University of Sheffield, 2009.

22. Soneda, T. and Nakano, K., "Investigation of vibrotactile sensation of human fingerpads by observation of contact zone", Tribology International; 43: 210-217, 2010.

23. Archard, J. F., "Elastic deformation and the laws of friction, Proceedings of the Royal Society of London", Series A, Mathematical and Physical Sciences; 243(1233): 190-205, 1957.

24. Moore, D. F., "The friction and lubrication of elastomers", Pergamon Press Inc., New York, 1972.

25. Johnson, K. L., Contact mechanics, Cambridge University Press, Cambridge, 1985.

26. EL-shimi, A. F., "In vivo skin friction measurements", Journal of the Society of Cosmetic Chemists; 28: 37-51, 1977.

27. Andreˊ, T., Leˊvesque, V., Hayward, V., Lefevre, P., Tonnard, J.L., "Effect of skin hydration on the dynamics of fingertip gripping contact", Journal of the Royal Society Interface", 8(64): 1574-1583, 2011

28. Liu, X., Lu, Z., Lewis, R., Carré, M.J. and Matcher, S.J., "Feasibility of using Optical Coherence Tomography to study the influence of skin structure on finger friction", Tribology International; 68: 34–44, 2013.

29. Liu, X., Gad, D., Lu, Z., Lewis, R., Carré, M.J. and Matcher, S.J., "The contributions of skin structural properties to the friction of human finger-pads", Proceedings of the IMechE Part J. Journal of Engineering Tribology; 229 (3): 294-311, 2015.

30. Hu, X., Maiti, R., Boadi, J., Li, W., Carré, M. J., Lewis, R., Franklin, S. E., Matcher, S. J., "Optical coherence elastography for human finger-pad skin deformation studies", Proc. SPIE Optical Elastography and Tissue Biomechanics III; 9710, 2016.

31. Lu, Z. H., Kasaragod, D. K. and Matcher, S. J., "Optic axis determination by fibre-based polarization-sensitive swept-source optical coherence tomography", Physics in Medicine and Biology; 56: 1105-1122, 2011.

32. Tang, W., Ge, S. R., Zhu, H., Cao, X. C. and Li, N., "The influence of normal load and sliding speed on frictional properties of skin", Journal of Bionic Engineering; 5: 33-38, 2008.

33. Zhang, M. and Mak, A. F. T., "In vivo friction properties of human skin", Prosthetics and Orthotics International; 23: 135-141, 1999.

34. Delalleau, A., Josse, G. Lagarde, J. M. Zahouani, H. and Bergheau, J. M., "A nonlinear elastic behavior to identify the mechanical parameters of human skin in vivo", Skin Research and Technology; 14: 152, 2008.

35. Hendriks, F. M., Mechanical behaviour of human epidermal and dermal layers in vivo, PhD Thesis. Technische Universiteit, Eindhoven; 2005.

36. Silver, F. H., Freeman, J. W. and DeVore, D., "Viscoelastic properties of human skin and processed dermis", Skin Research and Technology; 7: 18–23, 2001.

37. Holzapfel, G. A., Biomechanics of soft tissues: handbook of material behaviour. Available at http://www.biomech. tugraz.at/papers/report7.pdf 2000: 12.

38. Tomlinson, S. E., Lewis, R. and Carré, M. J., "Review of the frictional properties of finger-object contact when gripping", Proceedings of the IMechE Part J. Journal of Engineering Tribology; 221: 841-850, 2007.

39. Xydas, N. and Kao, I., "Modeling of contact mechanics and friction limit surface for soft fingers in robotics, with experimental results", International Journal of Robotic Research; 18(8): 941–950, 1999.

40. Terekhov, A. V. and Hayward, V., "Minimal adhesion surface area in tangentially loaded digital contacts", Journal of Biomechanics; 44: 2508-2510, 2011.